International Journal of Greenhouse Gas Control 30 (2014) 125–132

Contents lists available at ScienceDirect

International Journal of Greenhouse Gas Control

journal homepage: www.elsevier.com/locate/ijggc

Time-dependent electrochemical behavior of carbon steel in MEA-based CO_2 capture process

Yong Xiang, Maocheng Yan, Yoon-Seok Choi*, David Young, Srdjan Nesic

Institute for Corrosion and Multiphase Technology, Department of Chemical and Biomolecular Engineering, Ohio University, 342 West State Street, Athens, OH 45701, USA

ARTICLE INFO

Article history:
Received 19 September 2013
Received in revised form 28 August 2014
Accepted 6 September 2014

Keywords:
CO_2 capture
CO_2 corrosion
MEA
Carbon steel
Time-dependent
Electrochemical measurement

ABSTRACT

Time-dependent electrochemical behavior of carbon steel was evaluated in CO_2-loaded monoethanolamine (MEA) solutions in simulated carbon capture environments. Tests were conducted in 30 wt.% MEA solution with different combinations of controlling factors (oxygen [O_2], heat stable salts [HSS], flow and temperature) for 7 days. Corrosion behavior of carbon steel was evaluated by using electrochemical techniques (linear polarization resistance [LPR] and potentiodynamic polarization measurements), weight loss method and surface analytical techniques. Solution pH and ferrous/ferric ion concentration were also measured to monitor the change of water chemistry with time. The results showed that the corrosion rate of carbon steel decreased with time and then stabilized to very low values in the MEA/CO_2 condition. XPS characterization revealed formation of a very thin protective $FeCO_3$ layer on the surface, as well as adsorption of MEA. However, when O_2 was present in the system, the corrosion rates remained at relatively high values, further increasing with flow. The presence of HSS resulted in a higher corrosion rate at the initial stage, but had a minimal effect on the corrosion rate for longer time exposure. Temperature had a slight effect on the corrosion rate because the solubility of CO_2 and O_2 decreases with increasing temperature.

1. Introduction

Emissions from fossil fuel-fired power plants are a significant carbon dioxide (CO_2) source, a primary greenhouse gas. This accounts for approximately 30% of total worldwide CO_2 emissions (Aaron and Tsouris, 2005). Carbon capture and storage (CCS) is regarded as one of the most promising ways to mitigate global climate change problems.

The first step for the CCS process is that CO_2 needs to be captured from the flue gas in power plants. Alkanolamine-based capture solutions are the most widely used industrial solvents for acid gas removal (e.g., natural gas treatment). Consequently, they are a promising way to capture the abundant CO_2 for the purpose of CCS (Soosaiprakasam and Veawab, 2008). However, removing CO_2 with alkanolamine-based solvents from the flue gas has its own problems, e.g., corrosion (Khorrami et al., 2008; Macnab and Treseder, 1971). Monoethanolamine (MEA, HO–CH_2–CH_2–NH_2 [C_2H_7NO]) is the most widely used solvent for acid gas removal because of its high adsorption capacity and its capability to remove large volumes of CO_2 at a fast rate. However, MEA is regarded as the most corrosive alkanolamine used in flue gas treatment (Dupart et al., 1993b; Moser et al., 2011). In addition to forming an ammonium salt, it reacts with CO_2 to form carbamate. Carbamate has significant impact on the corrosiveness of the amine solution (Danckwerts, 1979; Mondal et al., 2012):

Carbamate ($C_3H_6NO_3^-$) formation

$$C_2H_7NO + CO_2 \leftrightarrow C_3H_6NO_3^- + H^+ \quad (1)$$

Protonation of MEA ($C_2H_8NO^+$)

$$C_2H_7NO + H^+ \leftrightarrow C_2H_8NO^+ \quad (2)$$

Overall reaction is as follows:

$$2C_2H_7NO + CO_2 \leftrightarrow C_3H_6NO_3^- + C_2H_8NO^+ \quad (3)$$

Both uniform and localized corrosion, such as pitting, erosion, galvanic, stress corrosion cracking, and intergranular corrosion, have been discovered at the location of the absorber, regenerator, rich-lean heat exchanger and reboiler (Dupart et al., 1993a; Veawab et al., 1999).

Corrosiveness of the CO_2-loaded MEA solution also depends on various factors such as temperature, presence of heat stable salts (HSS), oxygen (O_2), solution turbulence, etc. Temperature is

* Corresponding author. Tel.: +1 740 593 9944; fax: +1 740 593 9949.
E-mail address: choiy@ohio.edu (Y.-S. Choi).

http://dx.doi.org/10.1016/j.ijggc.2014.09.003
1750-5836/

regarded as one of the most important factors on the corrosion rate (Kittel et al., 2012). Temperature has an exponential effect on the corrosion rate, since the electrochemical reactions involved are thermally activated (Kittel et al., 2012). The temperature for absorber condition is around 50 °C in the real CO_2 capture plant, while it is around 120 °C for the stripper (Kittel et al., 2009).

The HSS, typical degradation products of the amines, can promote corrosion in the systems because they increase the conductivity of amine solutions (Rooney and DuPart, 2000). Furthermore, this can decrease the CO_2 absorption capacity because of the irreversible reaction with the amine (Rooney et al., 1996).

Flow and O_2 contamination are also important factors relating to the corrosion behavior. The presence of flow causes a higher corrosion rate due to the enhancement of the transport rates of corroding agents between the metal surface and bulk environment (Soosaiprakasam and Veawab, 2008). O_2 has been found to degrade alkanolamine, forming carboxylic and glycolic acids, as well as oxalate, which lead to HSS formation (Rooney and DuPart, 2000). In addition, when O_2 is present, an additional cathodic reaction is involved to oxidize the iron (Veawab and Aroonwilas, 2002).

MEA concentration was reported to have minimal effect on the corrosion rate (Kittel et al., 2012).

There are extensive research data available in the open literature on the effects of the above mentioned factors on the corrosion mechanism of carbon steel in CO_2-loaded MEA systems under pilot-scale CO_2 capture conditions (Cousins et al., 2013; Kittel et al., 2009; Moser et al., 2011) as well as laboratory based conditions (Kladkaew et al., 2009b; Martin et al., 2012; Soosaiprakasam and Veawab, 2008; Tanthapanichakoon et al., 2006). However, the corrosion behavior was evaluated by short-term electrochemical measurements or long-term weight loss measurements which provide average corrosion rate data. There are no previous reports concerning the time-dependent corrosion behavior of carbon steel in CO_2-loaded MEA solutions under different combinations of the aforementioned controlling factors.

In the present study, time-dependent electrochemical behavior of carbon steel in CO_2-loaded MEA (30 wt.%) solution was studied at ambient pressure, simulating the absorber and rich–lean heat exchanger conditions. The current study is focused on investigating the effect of O_2, HSS, flow and temperature on the changes of corrosion rate with time (7 days). The corrosion rates were measured by weight loss and electrochemical methods (open-circuit potential [OCP], linear polarization resistance [LPR] and potentiodynamic polarization measurements). Surface analytical techniques (scanning electron microscopy [SEM], energy dispersive X-ray spectroscopy [EDS] and X-ray photoelectron spectroscopy [XPS]) were also applied to obtain the surface morphology and chemical composition of corrosion products. In addition, solution pH and ferrous/ferric ion concentration were also measured to monitor the change of water chemistry with time.

2. Material and methods

2.1. Material and solution

Carbon steel (ASTM A36) was used in the present study, with a chemical composition of 0.23% C, 0.79% Mn, 0.29% Cu, 0.20% Si, 0.02% P, 0.03% S, and balance (98.44%) Fe. It was machined into two different specimen types: a rectangular type with a size of 2.54 cm by 1.25 cm by 0.5 cm for weight loss measurement and surface analysis, and a cylindrical type 1.3 cm in diameter and 1.3 cm in height for electrochemical measurements. The specimen surface was grounded to a 600-grit finish using silicon carbide (SiC) paper, then cleaned with isopropyl alcohol in an ultrasonic bath and dried. Before the experiments, the weights of the samples were measured by electronic balance with an accuracy of 0.1 mg, and the dimensions of samples were exactly measured by a Vernier caliper.

An aqueous solution of 30 wt.% MEA was prepared from a 99% MEA reagent and deionized (DI) water. Before each experiment, different gas mixtures (0.12 bar CO_2 or 0.12 bar CO_2 + 0.06 bar O_2, with N_2 as the balance gas in each case) were sparged into the test solution, depending on the test conditions. The CO_2 loading at 50 °C was around 0.53 mol CO_2/mol amine, while at 80 °C, it was around 0.39 mol CO_2/mol amine, calculated from the literature data (Jou et al., 1995). The dissolved oxygen concentration can be obtained from the literature data (Rooney and Daniels, 1998). In the current test conditions, the dissolved oxygen concentration was 1.5 ppmw at 50 °C, while it was 0.9 ppmw at 80 °C. The effect of water vapor pressure under different temperature conditions was considered when estimating both CO_2 loading and O_2 solubility. In order to achieve equilibrium, the solution was sparged with test gases for at least 12 h before the test, and it was continuously sparged during the experiment.

Bicine, formate and sulfate were selected for the HSS because they are the products of amine degradation reactions with CO_2, O_2 or associated with the presence of trace contaminants (SO_x). Bicine (*N*,*N*-bis(2-hydroxyethyl)glycine) has been reported as a common degradation product of MEA solutions (Bosen and Bedell, 2004). Formate is the primary degradation product from the oxidation of MEA (Rooney et al., 1998). Sulfate is the reaction product of SO_2 and O_2 in alkanolamine (Zhou et al., 2012). Formic acid and sulfuric acid were used to generate formate and sulfate, respectively, in the MEA solution. The total concentration of HSS was fixed at 15,800 ppm.

2.2. Experimental setup

Corrosion tests were carried out in a 2 L glass cell at different temperatures (50 and 80 °C). Fig. 1 shows a schematic of the experimental setup for the corrosion tests. The test rig consists of glass cell, condenser, hot plate equipped with temperature controller, gas supply set, rotator for testing under flowing condition, pH meter (Oakton pH 11, ±0.01) and Gamry potentiostat (REF 600 model). A three-electrode corrosion system was used (counter electrode, CE: platinum wire; reference electrode, RE: saturated silver/silver chloride [Ag/AgCl] electrode; working electrode, WE: carbon steel A36). Before running each corrosion test, the potential of the reference electrode was compared with the standard calomel electrode for calibration purposes, and the pH probe was also calibrated in pH 7 and pH 10 buffer solutions at the different test temperatures (50 °C and 80 °C). All the tests were conducted for 7 days under ambient pressure.

Test conditions are shown in Table 1, which were established in order to investigate the effect of O_2, HSS, flow and temperature on the corrosion of carbon steel in an aqueous MEA solution.

2.3. Methods

The corrosion properties of carbon steel were evaluated with time by LPR measurement, and potentiodynamic polarization tests were performed at the end of each test. In addition, ferrous (Fe^{2+})/ferric (Fe^{3+}) ion concentrations and solution pH were measured periodically in order to monitor changes in water chemistry with time. The combined Fe^{2+}/Fe^{3+} concentrations were measured from solution samples by Thermo Scientific GENESYS 10 Vis Spectrophotometer with iron phenanthroline reagent (FerroVer).

LPR measurements were performed within ± 10 mV with respect to the corrosion potential with a scan rate of 0.166 mV/s. Using the polarization resistance (R_p) obtained from LPR measurements, the corrosion current density (i_{corr}) was calculated using

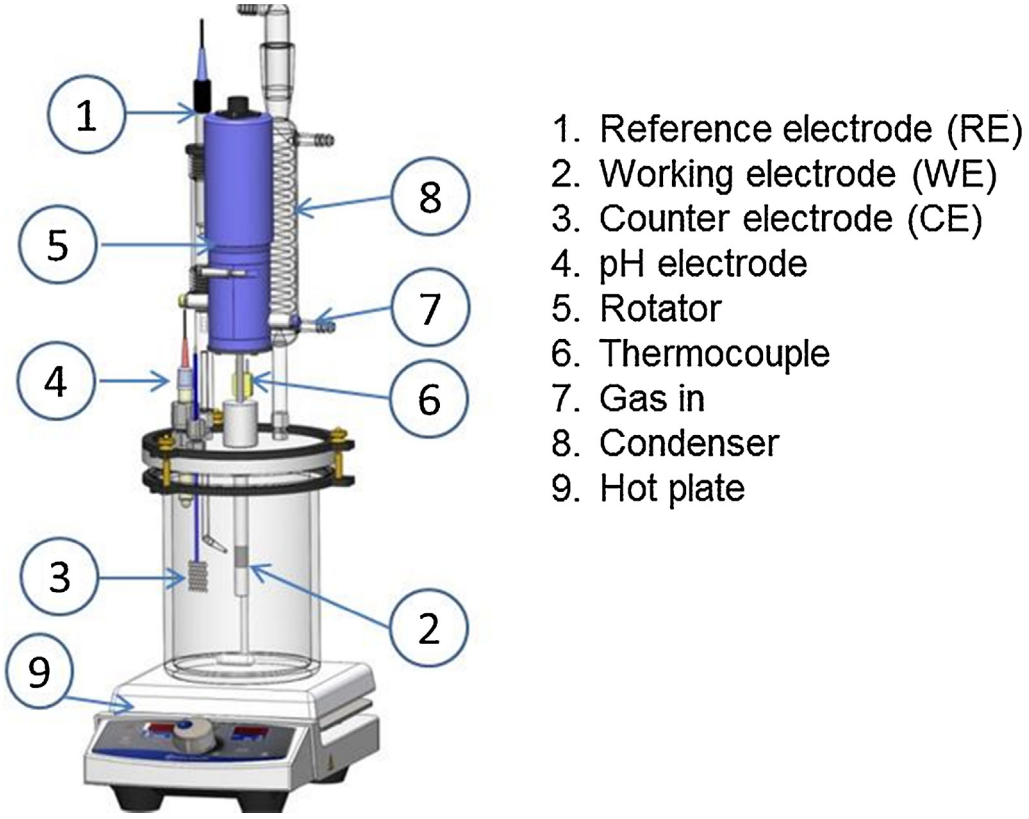

Fig. 1. Schematic of experimental setup for MEA corrosion tests.

Eq. (4) (Stern and Geary, 1957), and the resulting i_{corr} yields the corrosion rate using Eq. (5) (Dean, 1971):

$$i_{corr} = \frac{B}{R_p} = \frac{\beta_a \times \beta_c}{2.3 \times R_p \times (\beta_a + \beta_c)} \quad (4)$$

$$\text{corrosion rate}\left(\text{mm/y}\right) = \frac{0.00327 \times i_{corr}\left(\mu\text{A/cm}^2\right) \times \text{EW(g)}}{\text{dnsity}\left(\text{g/cm}^3\right)} \quad (5)$$

where β_a is the anodic Tafel constant, β_c is the cathodic Tafel constant, 0.00327 is a constant used for dimension and time conversion factor, and EW is the equivalent weight in grams. In the present study, 0.022 V/decade was used as the B value (Jones, 1996). Potentiodynamic polarization tests were carried out at the end of the test. The specimen was scanned potentiodynamically at a rate of 0.166 mV/s.

The corrosion rates were also determined by weight-loss method. At the beginning of each test, 4 specimens were inserted in the same glass cell where the electrochemical test was conducted. One specimen was removed for weight loss analysis on each of the following days: 1, 3, 5 and 7, and cleaned with the Clarke solution (20 g antimony trioxide + 50 g stannous chloride and hydrochloric acid to make 1000 mL) (ASTM, 1999). The specimens were then rinsed in distilled water, dried and weighed to 0.1 mg. The corrosion rate can be calculated by the following equation (ASTM, 1994):

$$\text{corrosion rate}\,(\text{mm/y}) = \frac{8.76 \times 10^4 \times \text{weight loss(g)}}{\text{area}\,(\text{cm}^2) \times \text{density}(\text{g/cm}^3) \times \text{time(h)}} \quad (6)$$

After the experiment, the weight loss specimen from the 7th day was used for additional ex situ analyses before cleaning with the Clarke solution. The specimen was withdrawn from the test cell, rinsed with DI water and isopropyl alcohol, and then dried. The morphology and compositions of corrosion products were analyzed with SEM, EDS, and XPS.

3. Results and discussion

3.1. Effect of O_2 and HSS

Fig. 2 shows the variations of corrosion rate and OCP with time for 30 wt.% MEA/12% CO_2 (MEA/CO_2), 30 wt.% MEA/12%

Table 1
Test conditions for the corrosion tests of carbon steel in MEA systems.

Test no.	CO_2 concentration (v%)	O_2 concentration (v%)	Rotation speed (rpm)	Temperature (°C)	HSS*
1	12	0	0	50	No
2	12	6	0	50	Yes
3	12	6	0	50	No
4	12	6	1000	50	No
5	12	0	1000	50	No
6	12	6	0	80	No

* HSS: 3.0×10^3 ppmw sulfuric acid [H_2SO_4] + 2.8×10^3 ppmw formic acid [HCOOH] + 1.0×10^4 ppmw bicine [$C_6H_{13}NO_4$].

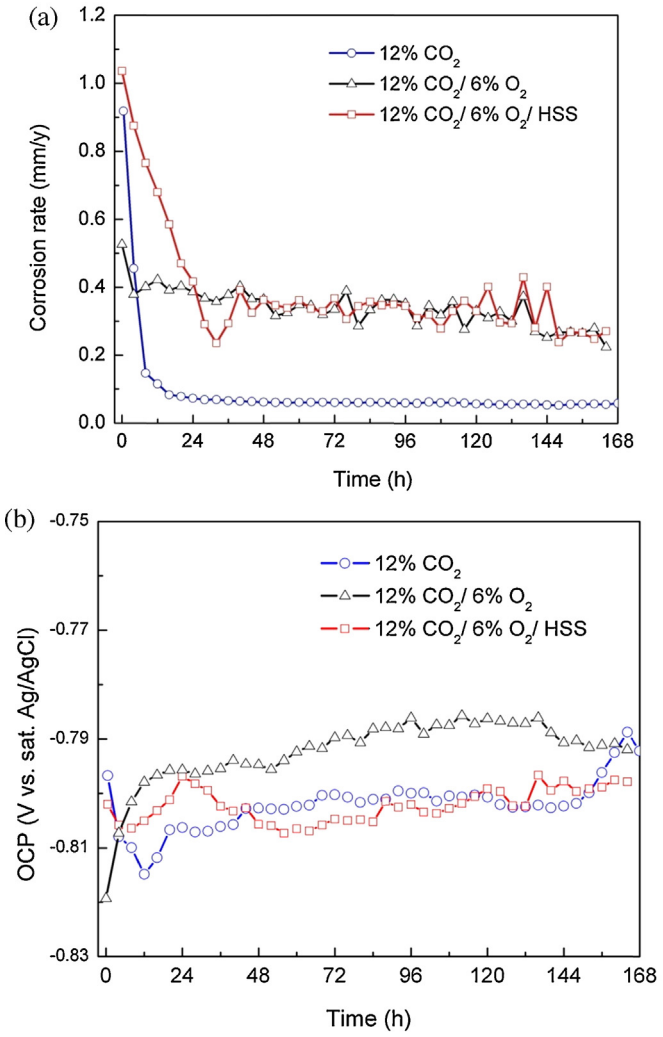

Fig. 2. Variations of (a) corrosion rate and (b) OCP of carbon steel in MEA systems with different test conditions.

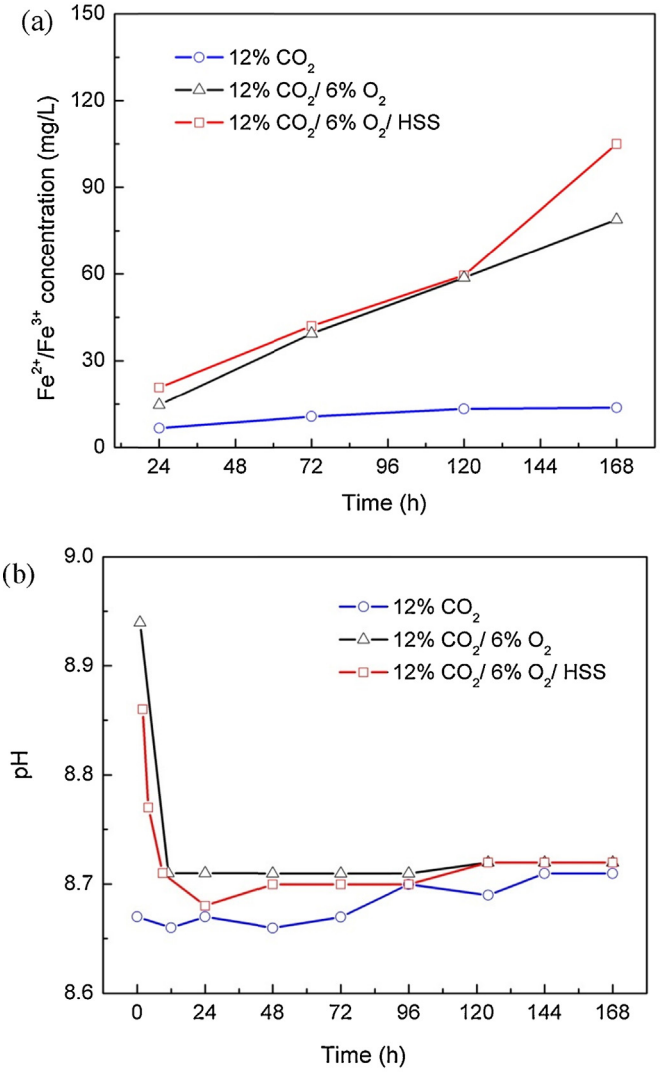

Fig. 3. Variations of (a) Fe^{2+}/Fe^{3+} concentrations and (b) MEA solution pH with different test conditions.

CO_2/6% O_2 (MEA/CO_2/O_2) and 30 wt.% MEA/12% CO_2/6% O_2/HSS (MEA/CO_2/O_2/HSS) at 50 °C. For all three conditions, the OCP changed by less than 30 mV during 7 days, and there is little difference in each condition at the end of the test. However, as shown in Fig. 2(a), the corrosion rates decreased for the first 24–48 h and then stabilized in the MEA/CO_2 and MEA/CO_2/O_2/HSS conditions whereas it maintained the initial value throughout the test periods with MEA/CO_2/O_2. At the beginning of the test, the relative corrosiveness of systems was ranked as: MEA/CO_2/O_2/HSS > MEA/CO_2 > MEA/CO_2/O_2, whereas it was changed to: MEA/CO_2/O_2/HSS ≈ MEA/CO_2/O_2 > MEA/CO_2 at the end of the test. The corrosion rate for the MEA/CO_2/O_2/HSS condition was high throughout the initial 24 h, but it decreased with time and then showed almost the same values as the MEA/CO_2/O_2 condition. This indicates that it affects the initial corrosion behavior with given types and concentrations of HSS. It is also interesting to note that a rapid decrease in the corrosion rate can be seen for the MEA/CO_2 condition, reaching a very low corrosion rate (≤0.1 mm/y) which may be attributed to the formation of a protective iron carbonate ($FeCO_3$) layer, the usual CO_2 corrosion product (Nesic, 2007; Yan et al., 2012).

The measured Fe^{2+}/Fe^{3+} concentrations and pH are shown in Fig. 3. The Fe^{2+}/Fe^{3+} concentrations increased with time for MEA/CO_2/O_2 and MEA/CO_2/O_2/HSS systems as a result of the continuous anodic dissolution of carbon steel. For the MEA/CO_2 system, Fe^{2+}/Fe^{3+} concentrations increased slightly during the test. The solution pH values decreased after 24 h for MEA/CO_2/O_2 and MEA/CO_2/O_2/HSS conditions and stabilized at similar values, whereas it slightly increased with time for the MEA/CO_2 condition. By comparison of Figs. 2(a) and 3(b), there is no obvious relationship between the corrosion rate and the solution pH.

The corrosion rates obtained by the weight loss measurements are shown in Fig. 4. The corrosion rates measured by weight loss show a similar trend with the results of LPR measurements, indicating that the presence of HSS enhanced the corrosion rate mainly at the initial stage of the corrosion process.

Based on the results of LPR and weight loss measurements, it is important to note that using the initial corrosion rate measured from electrochemical techniques or using the average corrosion rate measured from weight loss technique may give a false impression of the long term effect of controlling parameters (CO_2, HSS and O_2) on the corrosion rate in a real CO_2 capture plant.

Fig. 5 shows the effect of O_2 and HSS on the polarization behavior of carbon steel after 7-day exposure. It shows typical active-passive corrosion behavior for all three conditions. The addition of O_2 and HSS had no significant impact on the anodic process in the active region (−0.8 V to −0.6 V); however, it remarkably enhanced the cathodic process (−0.8 to −1.0 V) by involving new cathodic reactions (for example, O_2 reduction) in the corrosion process. When

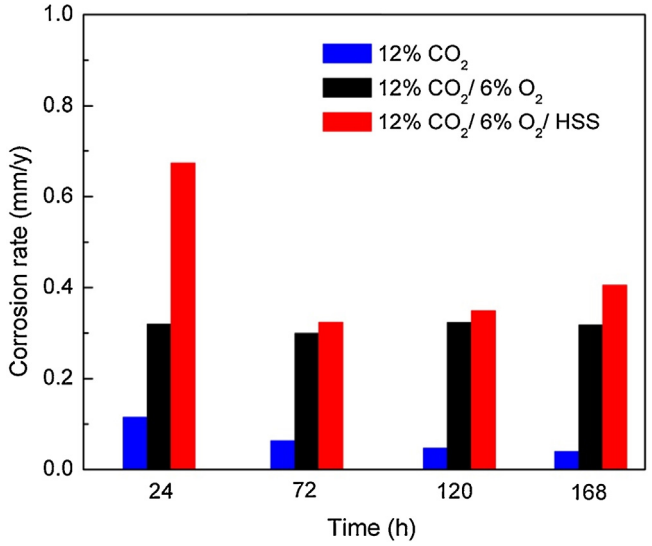

Fig. 4. Variation of corrosion rates of carbon steel with time measured from weight loss method in MEA systems.

carbon steel is exposed to a MEA/CO_2/H_2O environment, the electrochemical reactions occurring simultaneously at the steel surface are anodic dissolution of iron and reduction of the various cathodic species (Veawab and Aroonwilas, 2002):

Anodic (oxidation) reaction:

$$Fe \rightarrow Fe^{2+} + 2e^- \quad (7)$$

Cathodic (reduction) reactions:

$$2HCO_3^- + 2e^- \rightarrow 2CO_3^{2-} + H_2 \quad (8)$$

$$2H_3O^+ + 2e^- \rightarrow 2H_2O + H_2 \quad (9)$$

$$2H_2O + 2e^- \rightarrow 2OH^- + H_2 \quad (10)$$

When O_2 is present in the system, an additional cathodic reaction is involved to oxidize the iron as shown in Eq. (11) (Garcia-Arriaga et al., 2010; Kladkaew et al., 2009a,b):

$$O_2 + 2H_2O + 4e^- \rightarrow 4OH^- \quad (11)$$

In the passive region (−0.5 to 0.0 V), the presence of O_2 and HSS increased the passive current density (i_{pass}), indicating that the presence of O_2 and HSS reduced the protectiveness ability of the corrosion product layer covering the metal surface. In addition, the presence of HSS increased the critical current density (i_{crit}) in the active-passive transition region (−0.6 to −0.5 V). This implies that the mechanism of iron dissolution in the presence of HSS might have altered due to the iron chelating effect of bicine (Bosen and Bedell, 2004; Lawson et al., 2003).

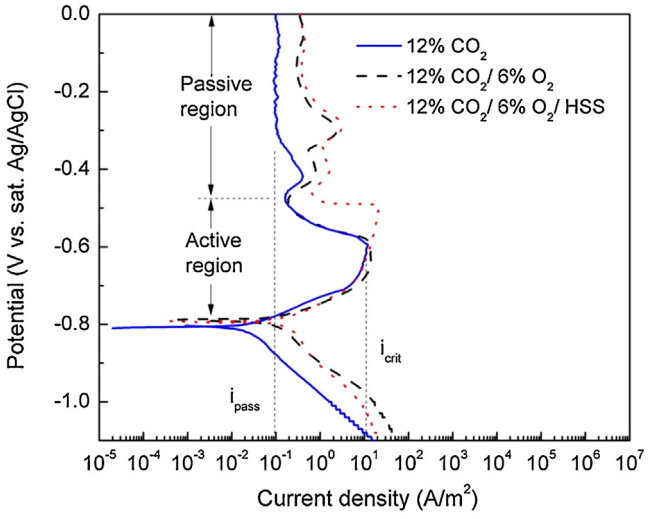

Fig. 5. Polarization curves of carbon steel in MEA systems with O_2 and HSS (after 7-day exposure).

Fig. 6 shows SEM images and EDS spectra of the corroded surface of the samples after 7-day exposure in MEA systems with different test conditions. The polishing marks are clearly visible for the MEA/CO_2 condition after 7-day exposure (Fig. 6(a)), indicating that the corrosion under this condition was minimal. However, for MEA/CO_2/O_2 and MEA/CO_2/O_2/HSS conditions, there seem to be some porous corrosion products on the sample surface. Since A36 carbon steel has a ferritic–pearlitic (*F*/*P*) microstructure, the dark and bright regions represent the ferrite phase and pearlite phase, respectively (Choi et al., 2010). EDS analysis also detected more carbon content at the bright region, indicating the presence of iron carbide (Fe_3C) which accumulated on the steel surface due to a preferential dissolution of ferrite (Mora-Mendoza and Turgoose, 2002).

As shown in Fig. 2(a), a very low corrosion rate (≤0.1 mm/y) was measured in the MEA/CO_2 condition, demonstrating the possibility of forming a protective corrosion product on the steel surface. However, no corrosion product was obvious in the EDS analysis (Fig. 6(a)). In order to confirm the presence of corrosion product on the steel surface, XPS analysis was performed on the sample that had been exposed to the MEA/CO_2 system for 7 days. Fig. 7 shows the results of XPS analyses of the carbon steel surface for the MEA/CO_2 condition. Fe $2p_{3/2}$ (≈710.2 eV), C 1s (≈289.4 eV) and O 1s (≈531.9 eV) peaks were detected, which are consistent with the presence of $FeCO_3$ (Heuer and Stubbins, 1999). In addition, a N 1s (≈400.3 eV) peak was also detected with peaks at 530.4 eV for O 1s and 286.0 eV for C 1s, indicating that MEA or carbamate chemically adsorbed on the steel surface. It is known that MEA acts as an inhibitor that adsorbs on the steel surface and inhibits the further fast corrosion of steel (Andreeva et al., 2002; Trace, 1981). Based on this result, it was confirmed that a thin layer of $FeCO_3$ had precipitated and MEA had adsorbed on the steel surface to provide the observed corrosion protection in the MEA/CO_2 system.

3.2. Effect of flow

Fig. 8 shows the effect of flow on the corrosion rate of carbon steel with time for MEA/CO_2 and MEA/CO_2/O_2 conditions at 50 °C. For MEA/CO_2 condition, the influence of flow seems to be minimal, and the corrosion rates decreased with time and stabilized to low values for both stagnant and flowing conditions. However, the presence of flow increased the corrosion rate of carbon steel for the MEA/CO_2/O_2 condition because it can enhance the mass transport of O_2 toward the steel surface, and ultimately increases the corrosion rate.

Effect of flow on the polarization behavior of carbon steel is displayed in Fig. 9. The presence of flow had no significant impact on the anodic process in the active region (−0.8 V to −0.7 V); however, it shows significant increase in cathodic current densities for the MEA/CO_2/O_2 condition (−0.8 to −1.0 V). This confirms that the presence of flow in the MEA/CO_2/O_2 system increased the corrosion rate of carbon steel by accelerating the O_2 reduction reaction (Eq. (11)).

3.3. Effect of temperature

Fig. 10 shows the effect of temperature on the corrosion rate of carbon steel with time in the MEA/CO_2/O_2 condition. High temperature (80 °C) simulates the rich-lean heat exchanger condition,

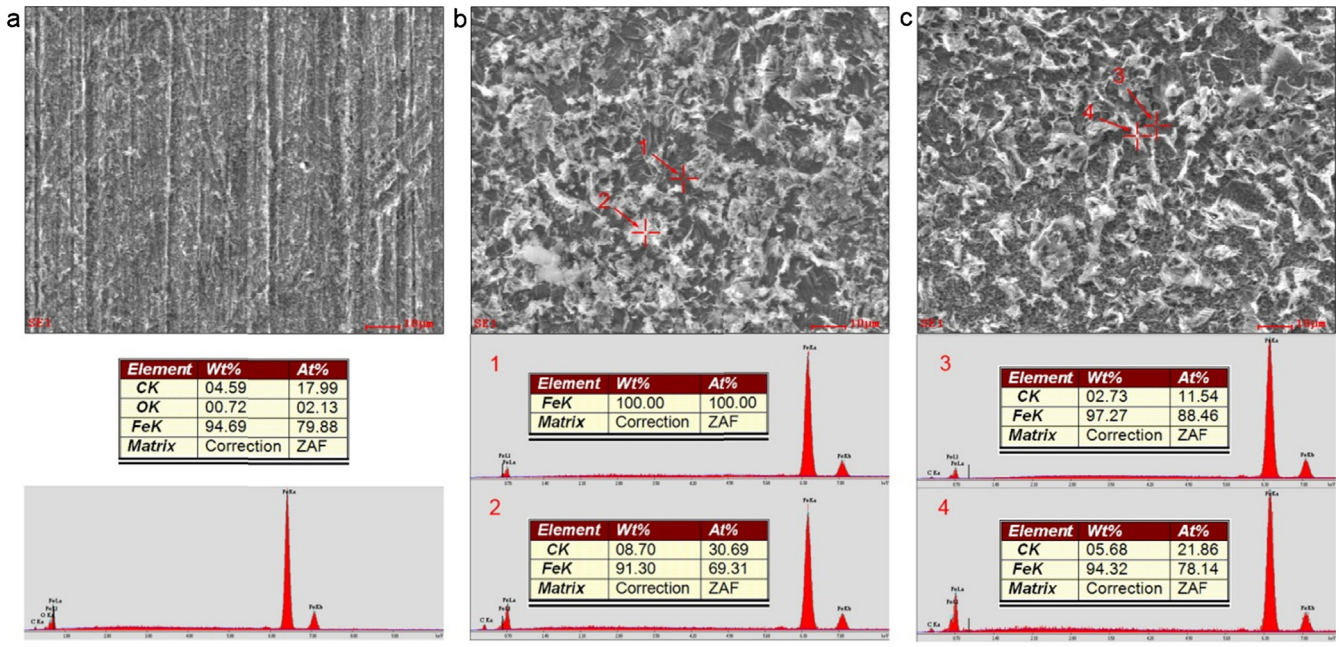

Fig. 6. SEM images and EDS spectra of the corroded surface of the samples after 7-day exposure: (a) MEA/CO_2, (b) MEA/CO_2/O_2, (c) MEA/CO_2/O_2/HSS.

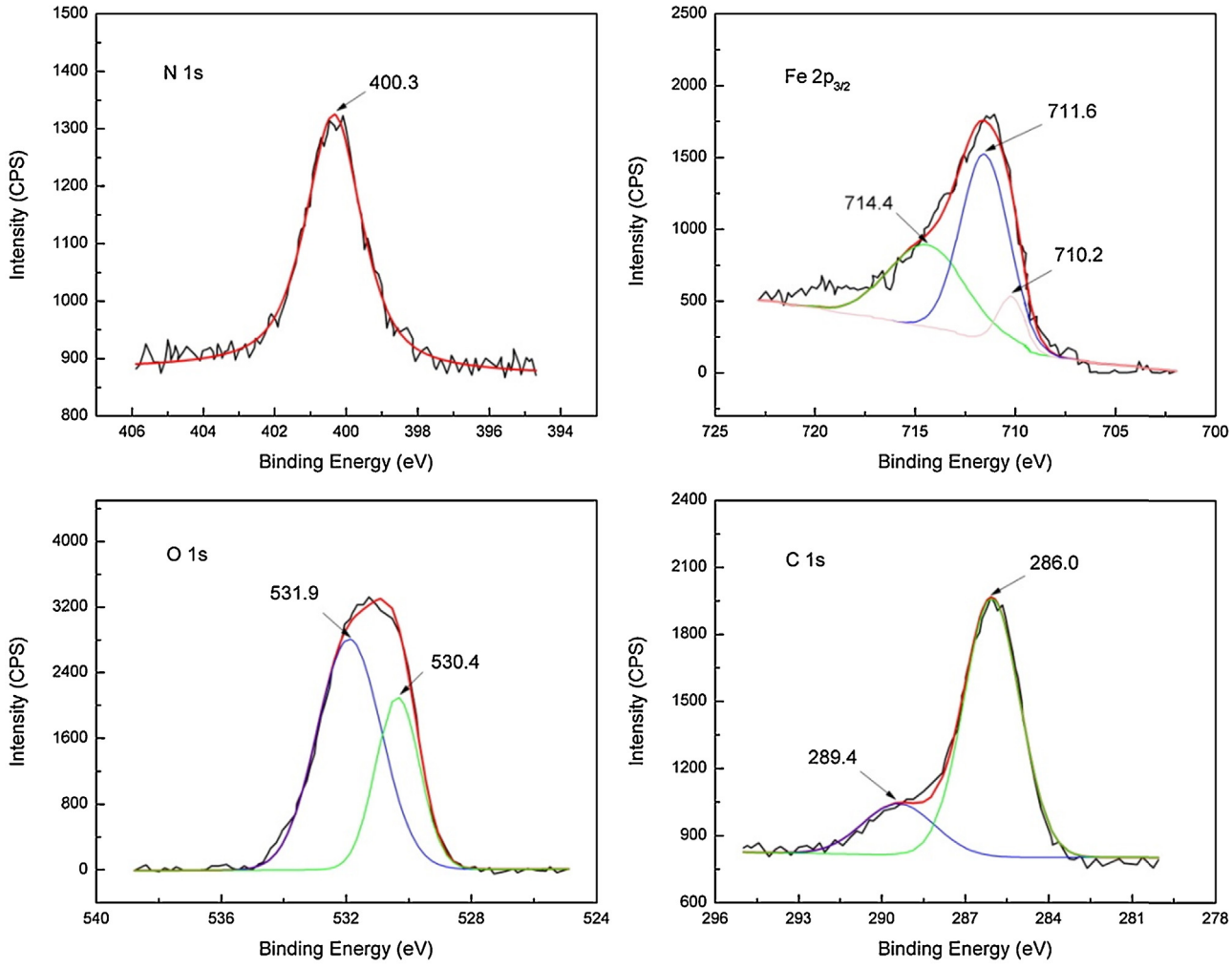

Fig. 7. XPS spectra of carbon steel exposed to MEA/CO_2 system for 7 days.

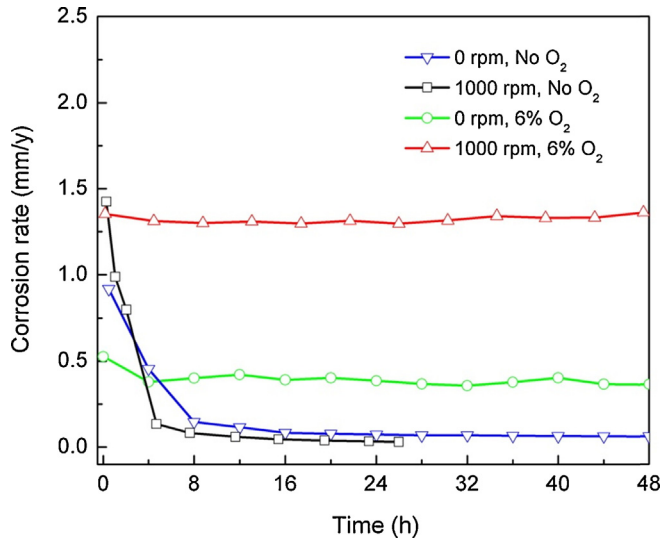

Fig. 8. Effect of flow on the corrosion rate of carbon steel with time under different conditions.

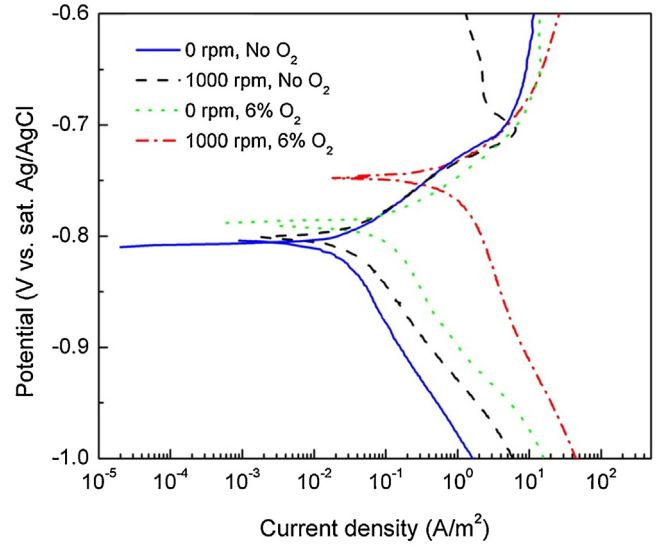

Fig. 9. Effect of flow on the polarization behavior of carbon steel under different conditions (after 7-day exposure).

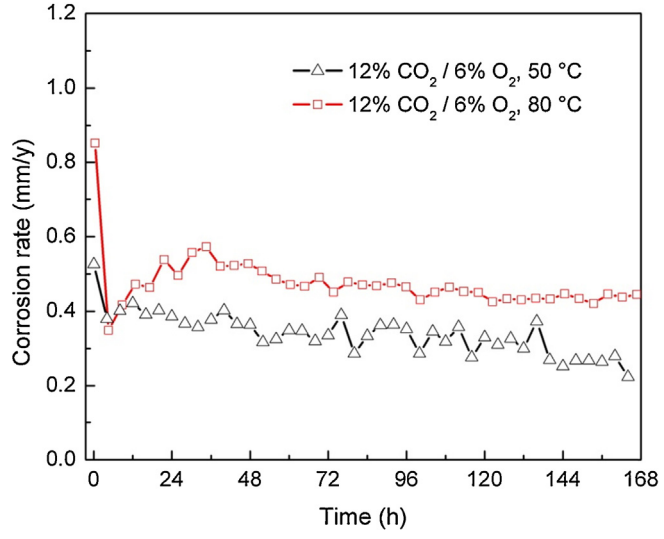

Fig. 10. Variations of corrosion rate in MEA/CO_2/O_2 system with different temperatures.

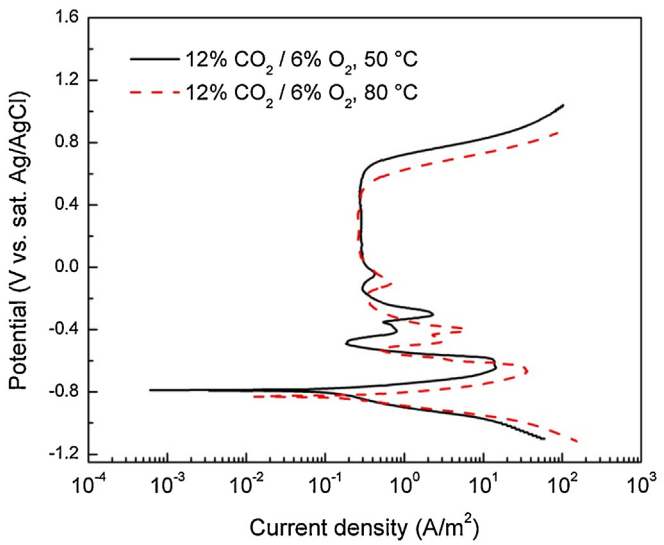

Fig. 11. Effect of temperature on the polarization behavior of carbon steel under MEA/CO_2/O_2 condition (after 7-day exposure).

which was reported as one of the most corrosive positions in the CO_2 capture plant (Gao et al., 2012; Kittel et al., 2009). The corrosion rate at 80 °C was higher than the corrosion rate at 50 °C, maintaining stable values with time at both temperatures. At the end of tests, the pH and the concentration of Fe^{2+}/Fe^{3+} values were 8.72 and 79 ppm at 50 °C, and 8.74 and 121 ppm at 80 °C.

The exponential effect of temperature on the corrosion rate, reported by Kittel et al. (2012), was observed only at the beginning of the test, but the corrosion rate at 80 °C decreased with time and showed slightly higher values than the corrosion rate at 50 °C throughout the test. This indicates that temperature affects mostly the initial corrosion behavior under this condition.

The polarization curves of carbon steel after 7-day exposure at different temperatures are illustrated in Fig. 11. The change in temperature had no significant impact on the cathodic process in the active region (−0.8 to −1.0 V) because the solubility of CO_2 and O_2 decreases with increasing temperature from 50 °C to 80 °C; however, it slightly enhanced the anodic process (−0.8 to −0.7 V), implying that iron dissolution reaction is accelerated by elevating temperature.

4. Conclusions

This work investigated the time-dependent corrosion behavior of A36 carbon steel in CO_2-loaded 30 wt.% MEA solution under different conditions. The following conclusions can be made:

(1) The corrosion rate of carbon steel decreased with time and then stabilized to very low value in the MEA/CO_2 condition due to the formation of a very thin protective $FeCO_3$ layer on the surface as well as the adsorption of MEA.
(2) When O_2 was present, the corrosion rates remained at relatively high values. The presence of HSS resulted in a higher corrosion rate at the initial stage, but had a minimal effect on the corrosion rate for longer time exposures.
(3) Flow enhances the mass transport of O_2 and had a significant effect on the corrosion rate.
(4) Temperature activates iron dissolution but has a slight effect on the corrosion rate because the solubility of CO_2 and O_2 decreases with increasing temperature.

Acknowledgement

The authors would like to thank the Russ College of Engineering and Technology in Ohio University for financial support of this research.

References

Aaron, D., Tsouris, C., 2005. Separation of CO_2 from flue gas: a review. Sep. Sci. Technol. 40, 321–348.

Andreeva, N.P., Bulgakova, R.A., Kuznetsov, Y.I., Sokolova, N.P., 2002. Adsorption of monoethanolamine on iron from a carbon dioxide atmosphere. Prot. Met. 38, 17–21.

ASTM, 1994. Standard Practice for Laboratory Immersion Corrosion Testing of Metals, Annual Book of ASTM Standards, vol. 03. 02, G 31. ASTM International, West Conshohocken, PA.

ASTM, 1999. Standard Practice for Preparing, Cleaning, and Evaluating Corrosion Test Specimens, Annual Book of ASTM Standards, vol. 03. 02, G 1. ASTM International, West Conshohocken, PA.

Bosen, S., Bedell, S.A., 2004. The Relevance of Bicine in Corrosion of Amine Gas Treating Plants, CORROSION/2004. NACE International, New Orleans, LA, USA (Paper no. 04481).

Choi, Y.S., Duan, D., Nesic, S., Vitse, F., Bedell, S.A., Worley, C., 2010. Effect of oxygen and heat stable salts on the corrosion of carbon steel in MDEA-based CO_2 capture process. Corrosion 66, 125004.

Cousins, A., Ilyushechkin, A., Pearson, P., Cottrell, A., Huang, S., Feron, P.H.M., 2013. Corrosion coupon evaluation under pilot-scale CO_2 capture conditions at an Australian coal-fired power station. Greenhouse Gases: Sci. Technol. 3, 169–184.

Danckwerts, P.V., 1979. The reaction of CO_2 with ethanolamines. Chem. Eng. Sci. 34, 443–446.

Dean, S.W., 1971. Handbook on Corrosion Testing and Evaluation. John Wiley, New York, NY.

Dupart, M.S., Bacon, T.R., Edwards, D.J., 1993a. Understanding corrosion in alkanolamine gas treating palnts. 1. Proper mechanism diagnosis optimizes amine operations. Hydrocarbon Process. 72, 75–80.

Dupart, M.S., Bacon, T.R., Edwards, D.J., 1993b. Understanding corrosion in alkanolamine gas treating plants. Hydrocarbon Process. 72, 89–94.

Gao, J., Wang, S., Sun, C., Zhao, B., Chen, C., 2012. Corrosion behavior of carbon steel at typical positions of an amine-based CO_2 capture pilot plant. Ind. Eng. Chem. Res. 51, 6714–6721.

Garcia-Arriaga, V., Alvarez-Ramirez, J., Amaya, M., Sosa, E., 2010. H_2S and O_2 influence on the corrosion of carbon steel immersed in a solution containing 3 M diethanolamine. Corros. Sci. 52, 2268–2279.

Heuer, J.K., Stubbins, J.F., 1999. An XPS characterization of $FeCO_3$ films from CO_2 corrosion. Corros. Sci. 41, 1231–1243.

Jones, D.A., 1996. Principles and Prevention of Corrosion. Prentice-Hall, Inc., Upper Saddle River, NJ.

Jou, F.Y., Mather, A.E., Otto, F.D., 1995. The solubility of CO_2 in a 30 mass percent monoethanolamine solution. Can. J. Chem. Eng. 73, 140–147.

Khorrami, M.R., Raeissi, K., Shahban, H., Torkan, M.A., Saatchi, A., 2008. Corrosion behavior of carbon steel in carbon dioxide-loaded activated methyl diethanol amine solution. Corrosion 64, 124–130.

Kittel, J., Idem, R., Gelowitz, D., Tontiwachwuthikul, P., Parrain, G., Bonneau, A., 2009. Corrosion in MEA units for CO_2 capture: pilot plant studies. Energy Procedia 1, 791–797.

Kittel, J., Fleury, E., Vuillemin, B., Gonzalez, S., Ropital, F., Oltra, R., 2012. Corrosion in alkanolamine used for acid gas removal: from natural gas processing to CO_2 capture. Mater. Corros.—Werkst. Korros. 63, 223–230.

Kladkaew, N., Idem, R., Tontiwachwuthikul, P., Saiwan, C., 2009a. Corrosion behavior of carbon steel in the monoethanolamine–H_2O–CO_2–O_2–SO_2 system. Ind. Eng. Chem. Res. 48, 8913–8919.

Kladkaew, N., Idem, R., Tontiwachwuthikul, P., Saiwan, C., 2009b. Corrosion behavior of carbon steel in the monoethanolamine–H_2O–CO_2–O_2–SO_2 system: products, reaction pathways, and kinetics. Ind. Eng. Chem. Res. 48, 10169–10179.

Lawson, G.L., Cummings, A.L., Mecum, S., 2003. Amine Plant Corrosion Reduced by Removal of Bicine. Gas Processors Association Annual Convention, San Antonio, TX, USA.

Macnab, A.J., Treseder, R.S., 1971. Materials requirements for a gas treating process. Mater. Prot. Perform. 10, 21–26.

Martin, S., Lepaumier, H., Picq, D., Kittel, J., de Bruin, T., Faraj, A., Carrette, P.-L., 2012. New amines for CO_2 capture IV. Degradation, corrosion, and quantitative structure property relationship model. Ind. Eng. Chem. Res. 51, 6283–6289.

Mondal, M.K., Balsora, H.K., Varshney, P., 2012. Progress and trends in CO_2 capture/separation technologies: a review. Energy 46, 431–441.

Mora-Mendoza, J.L., Turgoose, S., 2002. Fe_3C influence on the corrosion rate of mild steel in aqueous CO_2 systems under turbulent flow conditions. Corros. Sci. 44, 1223–1246.

Moser, P., Schmidt, S., Uerlings, R., Sieder, G., Titz, J.-T., Hahn, A., Stoffregen, T., 2011. Material testing for future commercial post-combustion capture plants—results of the testing programme conducted at the Niederaussem pilot plant. Energy Procedia 4, 1317–1322.

Nesic, S., 2007. Key issues related to modelling of internal corrosion of oil and gas pipelines—a review. Corros. Sci. 49, 4308–4338.

Rooney, P.C., Daniels, D.D., 1998. Oxygen solubility in various alkanolamine/water mixtures. Pet. Technol. Q. 3, 97–101.

Rooney, P.C., DuPart, M.S., 2000. Corrosion in alkanolamine plants: causes and minimization. In: CORROSION/2000, NACE.

Rooney, P.C., Bacon, T.R., DuPart, M.S., 1996. Effect of heat stable salts on MDEA solution corrosivity. Hydrocarbon Process. 75, 95–103.

Rooney, P.C., DuPart, M.S., Bacon, T.R., 1998. Oxygen's role in alkanolamine degradation. Hydrocarbon Process. 77, 109–113.

Soosaiprakasam, I.R., Veawab, A., 2008. Corrosion and polarization behavior of carbon steel in MEA-based CO_2 capture process. Int. J. Greenhouse Gas Control 2, 553–562.

Stern, M., Geary, A.L., 1957. Electrochemical polarization I. A theoretical analysis of the shape of polarization curves. J. Electrochem. Soc. 104, 56–63.

Tanthapanichakoon, W., Veawab, A., McGarvey, B., 2006. Electrochemical investigation on the effect of heat-stable salts on corrosion in CO_2 capture plants using aqueous solution of MEA. Ind. Eng. Chem. Res. 45, 2586–2593.

Trace, W.L., 1981. Condensate corrosion inhibition—a novel approach. Mater. Performance 20, 46–49.

Veawab, A., Aroonwilas, A., 2002. Identification of oxidizing agents in aqueous amine-CO_2 systems using a mechanistic corrosion model. Corros. Sci. 44, 967–987.

Veawab, A., Tontiwachwuthikul, P., Chakma, A., 1999. Corrosion behavior of carbon steel in the CO_2 absorption process using aqueous amine solutions. Ind. Eng. Chem. Res. 38, 3917–3924.

Yan, W., Deng, J., Li, X., Dong, X., Zhang, C., 2012. Effects of silty sand on CO_2 corrosion behavior of low-Cr tubing steel. Chin. Sci. Bull. 57, 927–934.

Zhou, S., Wang, S., Chen, C., 2012. Thermal degradation of monoethanolamine in CO_2 capture with acidic impurities in flue gas. Ind. Eng. Chem. Res. 51, 2539–2547.